Z. Phys. B – Condensed Matter 72, 391–398 (1988)

Condensed Matter
Zeitschrift für Physik B

Thermodynamic properties of the classical Heisenberg chain with nearest- and next-nearest-neighbor interactions

I. Harada* and H.J. Mikeska
Institut für Theoretische Physik, Universität Hannover, Federal Republic of Germany

Received April 7, 1988

Exact results for the thermodynamic quantities of the one-dimensional classical Heisenberg model with nearest- and next-nearest-neighbor exchange interactions are obtained by means of the numerical transfer matrix method. For a wide range of exchange constants, the system exhibits helical short-range order on which we focus our attention. We find that the Fourier-transformed spin correlation function shows a maximum with asymmetric shape at the characteristic wave-number $\pm q_m$ $(\neq 0, \pm\pi)$. The correlation length defined as the inverse of the width at $q=q_m$ obeys a simple scaling law and shows a power-law singularity at zero temperature. Results for the heat capacity and the susceptibility are also presented and discussed in connection with the helical short-range order.

1. Introduction

One-dimensional magnetic systems have attracted wide-spread interest during the past decade. Exact solutions for various classical spin chains as well as certain quantum spin chains play special roles for understanding characteristic phenomena occurring in real quasi-one-dimensional magnets. In some cases, not only qualitative but also quantitative comparisons between theoretical results and experimental ones have been made. Unfortunately, however, these are restricted to systems where only nearest-neighbor interactions are present. Recently, in connection with the so-called frustration effect, renewed interest has been paid to systems involving competing interactions. In this paper, we focus our attention on a classical spin chain with competing nearest-neighbor (nn) and next-nearest-neighbor (nnn) interactions (for the importance of quantum effects for systems with competing interactions see [1, 2]). It is well-known that in the classical spin chain, the antiferromagnetic nnn interaction leads to a helical spin order at zero temperature. At finite temperatures this helical order is destroyed by thermal fluctuations; however, a well-developed helical short-range order is responsible for unique phenomena at low temperatures.

In this paper we extend the transfer matrix method of the nn problem to allow for nnn interactions and study by using this method the nature of the helical short-range order of the system described by the following Hamiltonian:

$$H=\sum_{n=1}^{N}\{2J_1\mathbf{S}_n\cdot\mathbf{S}_{n+1}+2J_2\mathbf{S}_n\cdot\mathbf{S}_{n+2}\}, \tag{1}$$

where $\mathbf{S}_n$ is the classical unit vector at the $n-th$ site,

$$\mathbf{S}_n=(\sin\Theta_n\cos\Phi_n,\ \sin\Theta_n\sin\Phi_n,\ \cos\Theta_n), \tag{2}$$

and satisfies the periodic boundary condition, $\mathbf{S}_{n+N}=\mathbf{S}_n$. ($N$ is the number of sites in the chain.) The nn and the nnn exchange interaction constant are denoted, respectively, by J_1 and J_2 and are assumed to be antiferromagnetic ($J_1, J_2>0$) in this paper. We note that the factor of the spin magnitude $\sqrt{S(S+1)}$ is absorbed in the exchange interaction constants.

It is noted that the dynamic and static correlation functions of the system described by the Hamiltonian (1) have been studied by Monte Carlo simulations

* Permanent address: Department of Physics, Faculty of Science Kobe University, Rokkodai, Kobe, 657 Japan

[3], which have wide applicability but yield inevitable errors. Our results by the transfer matrix method are complementary since they are exact in the sense that we can improve them systematically to any desired degree but are restricted to the static quantities.

Now, we envisage the characteristics of our system. We first note that the ground state has a usual antiferromagnetic spin structure when the ratio $j \equiv J_2/J_1$ is smaller than 1/4 but is helimagnetic for $j > 1/4$. The helimagnet is characterized by its wavenumber Q which takes one of the following two values, $\pm \arccos(-1/4j)$, where in our units the lattice constant is equal to unity. This degeneracy called the chiral symmetry corresponds to the degeneracy of the clockwise and the counter-clockwise turn of spins. Then, it is conceivable that there occurs an excitation of the chiral domain wall, which separates domains of opposite chirality in the helical spin structure. In fact, it has already been found that in the planar chain with nn and nnn interactions the chiral domain wall dominates the thermodynamics at low temperatures [4]. However, in the present system the chirality vector defined by $\mathbf{K}_n = \mathbf{S}_n \times \mathbf{S}_{n+1}/|\sin Q|$ is a three dimensional vector, whereas it has only one component (pseudo-scalar) in the planar chain. Thus the effect of chiral domain walls is expected to be quite different from that in the planar model. Therefore it appears worthwhile to study the role of this type of excitations.

In the next section, we formulate the transfer matrix method by introducing the dual lattice with the dual spin defined by the relative angle between nn spins in the original lattice. Then we solve numerically the transfer-matrix integral equations and obtain the results for the internal energy, the heat capacity and the susceptibility. These will be presented in graphical form in Sect. 3. Finally we give concluding remarks in Sect. 4.

2. Formulation

2.1. Free energy

We develop in this section the transfer matrix method to obtain the thermodynamic properties of the classical Heisenberg chain with nn and nnn interactions described by the Hamiltonian (1) [5]. With the notation $t = k_B T/2J_1$, where k_B is the Boltzmann constant and T is the temperature, the partition function is written as

$$Z = \left(\prod_{n=1}^{N} \int \mathrm{d}\Omega_n \right) \exp\{ -\sum_n (\mathbf{S}_n \cdot \mathbf{S}_{n+1} + j \mathbf{S}_n \cdot \mathbf{S}_{n+2})/t \}, \quad (3)$$

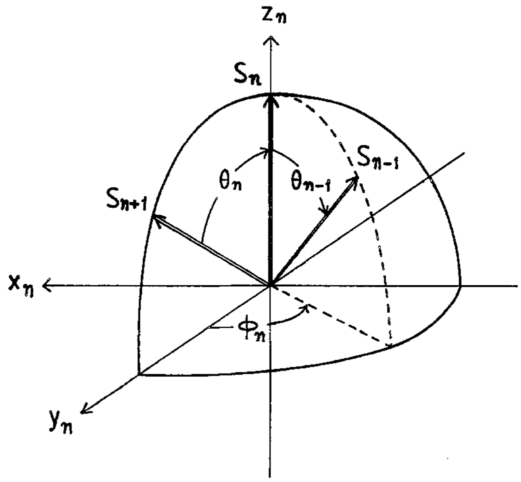

Fig. 1. Local coordinate system for the $n-th$ spin. The z_n axis is chosen parallel to $\mathbf{S}_n$ while the y_n axis is in the plane spanned by $\mathbf{S}_n$ and $\mathbf{S}_{n+1}$. Then, the angles, θ_n and ϕ_n, are defined, respectively, by the angle between $\mathbf{S}_{n+1}$ and $\mathbf{S}_n$ and by the angle between the components of $\mathbf{S}_{n+1}$ and of $\mathbf{S}_{n-1}$ projected onto the $x_n - y_n$ plane

where $\mathrm{d}\Omega_n$ is the volume element of the solid angle for the $n-th$ spin,

$$\mathrm{d}\Omega_n = \sin\Theta_n \, \mathrm{d}\Theta_n \, \mathrm{d}\Phi_n / 4\pi. \quad (4)$$

By an analogy with the dual transformation in the planar model [4], let us introduce a new set of the angles $\{\Theta_n, \phi_n\}$ (see Fig. 1). We choose the z_n axis parallel to $\mathbf{S}_n$ and the y_n axis in the plane spanned by $\mathbf{S}_n$ and $\mathbf{S}_{n+1}$. Thus, Θ_n is defined by the angle between $\mathbf{S}_{n+1}$ and $\mathbf{S}_n$ and the angle ϕ_n is defined by the angle between the components of $\mathbf{S}_{n-1}$ and of $\mathbf{S}_{n+1}$ projected onto the $x_n - y_n$ plane. In terms of these variables, Z is rewritten as

$$Z = \prod_{n=1}^{N} \{ \int 2 \, \mathrm{d}\Omega_n A(\theta_{n-1}, \theta_n; \phi_n) \}, \quad (5)$$

where

$$A(\theta_{n-1}, \theta_n; \phi_n) = (1/2) \exp\{ -(\cos\theta_{n-1} + \cos\theta_n)/2t - j(\cos\theta_{n-1}\cos\theta_n + \sin\theta_{n-1}\sin\theta_n \cos\phi_n)/t \}. \quad (6)$$

It is easy to see that the integration over ϕ_n results in the Bessel function of an imaginary argument. Changing integral variables from $\{\cos\theta_n\}$ to $\{x_n\}$, we obtain

$$Z = \prod_n \{ \int_{-1}^{1} \mathrm{d}x_n A_0(x_{n-1}, x_n) \}, \quad (7)$$

where we have defined A_0 and A_1 (which will be used later) by

$$A_m(x_{n-1}, x_n)=(1/2)\exp\{-(x_{n-1}+x_n)/2t-j x_{n-1} x_n/t\} \cdot I_m(-(j/t)\sqrt{(1-x_{n-1}^2)(1-x_n^2)}), \quad m=0, 1. \tag{8}$$

Here $I_m(z)$ is the modified Bessel function defined by the following integral,

$$I_m(z)=(1/2\pi)\int_{-\pi}^{\pi} \mathrm{d}\phi \exp(z\cos\phi)\cos m\phi. \tag{9}$$

Now, we introduce the following integral equation in order to perform the multiple integration over x_n's in (7):

$$\int_{-1}^{1} \mathrm{d}x_2 A_0(x_1, x_2)\psi_\alpha(x_2)=\lambda_\alpha \psi_\alpha(x_1), \tag{10}$$

where the eigenvalue λ_α and the eigenfunction ψ_α can be chosen as real numbers since the kernel $A_0(x_1, x_2)$ is real and symmetric with respect to x_1 and x_2. We solve this integral equation numerically by means of the Gaussian quadrature. Utilizing the well-known expansion of the kernel $A_0(x_1, x_2)$ with respect to λ_α and ψ_α,

$$A_0(x_1, x_2)=\sum_\alpha \lambda_\alpha \psi_\alpha(x_1)\psi_\alpha(x_2), \tag{11}$$

and employing the orthonormality relation,

$$\int_{-1}^{1} \mathrm{d}x\, \psi_\alpha(x)\psi_\beta(x)=\delta_{\alpha,\beta}, \tag{12}$$

where $\delta_{\alpha,\beta}$ is the Kronecker delta function, we obtain the final form of the partition function:

$$Z=\sum_\alpha (\lambda_\alpha)^N. \tag{13}$$

In the thermodynamic limit, $N\to\infty$, only the largest eigenvalue, λ_0, survives in the summation and the free energy per spin is given by

$$f=-t\ln\lambda_0. \tag{14}$$

The internal energy ε and the heat capacity C are obtained by differentiating f:

$$\varepsilon=-t^2\,\partial(f/t)/\partial t, \tag{15}$$

$$C=\partial\varepsilon/\partial t. \tag{16}$$

2.2. *Pair correlation function*

Probably the most interesting quantities to be calculated for our spin chain is the two-spin correlation function. However more effort than before is needed to obtain it because the scalar product of a pair of spins, $\mathbf{S}_n\cdot\mathbf{S}_{n+m}$, can not be expressed only by the angles (θ_n, ϕ_n) and $(\theta_{n+m}, \phi_{n+m})$ but depends on all the angles between the sites n and $n+m$. To see this, let us introduce the rotational operators,

$$R^z(\phi_n)=\begin{pmatrix} -\cos\phi_n & -\sin\phi_n & 0 \\ \sin\phi_n & -\cos\phi_n & 0 \\ 0 & 0 & 1 \end{pmatrix}, \tag{17}$$

which corresponds to a rotation around the z_n axis by the angle $\pi+\phi_n$ and

$$R^x(\theta_n)=\begin{pmatrix} 1 & 0 & 0 \\ 0 & \cos\theta_n & \sin\theta_n \\ 0 & -\sin\theta_n & \cos\theta_n \end{pmatrix}, \tag{18}$$

which corresponds to a rotation around the x_n axis by the angle θ_n. Then, the successive operation of these rotations, $T_n=R^x(\theta_{n-1})R^z(\phi_n)$, transforms the $n-th$ coordinate system to the $(n-1)-th$ coordinate system. (See Fig. 1.) We need the z-component of $\mathbf{S}_{n+m}$ in the $n-th$ coordinate system to obtain the scalar product, $\mathbf{S}_n\cdot\mathbf{S}_{n+m}$. Noticing that each $\mathbf{S}_n$ is parallel to each z_n axis, we obtain

$$\mathbf{S}_n\cdot\mathbf{S}_{n+m}=(001)\left(\prod_{l=n+1}^{n+m} T_l\right)_{33}\begin{pmatrix}0\\0\\1\end{pmatrix}. \tag{19}$$

The correlation function defined by the thermal average of the spin product, $\langle\mathbf{S}_n\cdot\mathbf{S}_{n+m}\rangle$, involves again the multiple integrals including the matrices T_l:

$$W_m=(1/Z)\prod_{k=1}^{N}\{\int 2\,\mathrm{d}\Omega_k A(\theta_{k-1}, \theta_k; \phi_k)\} \cdot(001)\left(\prod_{l=n+1}^{n+m} T_l\right)_{33}\begin{pmatrix}0\\0\\1\end{pmatrix}. \tag{20}$$

Fortunately, the integrations over ϕ_k's are again separable and are easily related to A_m defined by (8):

$$(1/2\pi)\int \mathrm{d}\phi_k R^z(\phi_k)A(\theta_{k-1}, \theta_k; \phi_k) =\begin{pmatrix} -A_1(\theta_{k-1}, \theta_k) & 0 & 0 \\ 0 & -A_1(\theta_{k-1}, \theta_k) & 0 \\ 0 & 0 & A_0(\theta_{k-1}, \theta_k) \end{pmatrix}. \tag{21}$$

The diagonal form of this matrix as well as the block-diagonal form of R^x make our calculations rather simple: Since we need only the (3.3) element of the resultant matrix it is sufficient to deal with the 2×2 matrices $H(n-1, n)$,

$$H(n-1,n)=\{R^x(\theta_{n-1})\}^{1/2}\cdot\begin{pmatrix}-A_1(\theta_{n-1},\theta_n) & 0\\ 0 & A_0(\theta_{n-1},\theta_n)\end{pmatrix}\{R^x(\theta_n)\}^{1/2}, \tag{22}$$

with

$$\{R^x(\theta_n)\}^{1/2}=\begin{pmatrix}\cos(\theta_n/2) & \sin(\theta_n/2)\\ -\sin(\theta_n/2) & \cos(\theta_n/2)\end{pmatrix}. \tag{23}$$

Changing again the integral variables, we obtain

$$W_m=(1/\lambda_0^{m-1})\int dx_n\ldots\int dx_{n+m-1}\psi_0(x_n)\psi_0(x_{n+m-1})\cdot(01)\{R^x(x_n)\}^{1/2}\prod_{h=n}^{n+m-2}H(x_h,x_{h+1})\cdot\{R^x(x_{n+m-1})\}^{1/2}\begin{pmatrix}0\\1\end{pmatrix}. \tag{24}$$

To perform the multiple integration over x_n's we introduce the following integral equation:

$$\int dx_2\,H(x_1,x_2)\,u_\alpha(x_2)=\eta_\alpha u_\alpha(x_1). \tag{25}$$

As is easily realized, the kernel $H(x_1, x_2)$ is neither a symmetric matrix nor symmetric with respect to the arguments x_1 and x_2. Therefore it is necessary to consider its counterpart:

$$\int dx_2\,H^T(x_1,x_2)\,v_\alpha(x_2)=\eta_\alpha v_\alpha(x_1), \tag{26}$$

where H^T denotes the transposed matrix of H. Here $u_\alpha(v_\alpha)$ is a vector with two components, u_α^1 and u_α^2 (v_α^1 and v_α^2). The solutions of these integral equations have the following properties: *(1)* The two integral equations share the eigenvalues $\{\eta_\alpha\}$. *(2)* u_α and v_α satisfy the orthonormality relations,

$$\int dx\,v_\alpha^T(x)\,u_\beta(x)=\int dx\,u_{\alpha(x)}^T\,v_\beta(x)=\delta_{a,b}. \tag{27}$$

(3) Since H is not symmetric, the eigenvalues can be complex numbers. *(4)* When η_α, u_α and v_α are a solution their complex conjugates, η_α^*, u_α^* and v_α^*, are also a solution. The complex conjugate contributions from these solutions will guarantee the reality of the spin correlation function. Keeping this in mind, we expand the kernel H in terms of the eigenvalue and the eigenfunction with the result

$$H(x_1,x_2)=\sum_\alpha \eta_\alpha u_\alpha(x_1)\,v_\alpha^T(x_2). \tag{28}$$

Substituting (28) into (24) and using the orthonormality relation (27), we obtain

$$W_m=\sum_\alpha y_\alpha^{m-1}E_{0\alpha}F_{0\alpha},\qquad m\geqq 1 \tag{29}$$

where

$$y_\alpha=\eta_\alpha/\lambda_0, \tag{30}$$

$$E_{0\alpha}=\int_{-1}^{1}dx\,\psi_0(x)(01)\{R^x(x)\}^{1/2}u_\alpha, \tag{31}$$

$$F_{0\alpha}=\int_{-1}^{1}dx\,\psi_0(x)\,v_\alpha^T\{R^x(x)\}^{1/2}\begin{pmatrix}0\\1\end{pmatrix}. \tag{32}$$

Now it is straightforward to obtain the structure factor which is the Fourier-transformed spin correlation function:

$$S(q)=\sum_{m=-\infty}^{\infty}W_m e^{iqm}=1+2\sum_\alpha E_{0\alpha}F_{0\alpha}(\cos q-y_\alpha)/(1-2y_\alpha\cos q+y_\alpha^2). \tag{33}$$

$S(q)$ shows a maximum at $q=\pm q_m$ where q_m takes continuous values from π to $\pi/2$ depending on the temperature and the ratio j. The correlation length ξ is defined as the inverse of the width of $S(q)$ around $q=q_m$:

$$S(q)\cong S(q_m)/[1+\{\xi(q-q_m)\}^2]. \tag{34}$$

The dimensionless susceptibility is given by

$$\chi(q)=S(q)/t. \tag{35}$$

Before closing this section, we briefly describe how to calculate the correlation function for the chirality vector $\mathbf{K}$. To this end we introduce the susceptibility of the chirality

$$\chi^{KK}=(1/t)\sum_m\langle\mathbf{K}_n\cdot\mathbf{K}_{n+m}\rangle\exp(iqm)=(1/t\sin^2 Q)\sum_m\langle\sin\theta_n\sin\theta_{n+m}x_n\cdot x_{n+m}\rangle\exp(iqm), \tag{36}$$

where x_n is a unit vector having only an x-component in the $n-th$ coordinate system. Proceeding in an analogous way as above we obtain the result:

$$\chi^{KK}(q)=(1/t\sin^2 Q)\sum_\alpha G_\alpha^2(1-z_\alpha^2)/(1-2\cos q\,z_\alpha+z_\alpha^2), \tag{37}$$

where

$$z_\alpha=\zeta_\alpha/\lambda_0, \tag{38}$$

$$G_\alpha=\int dx\sqrt{1-x^2}\,\psi_0(x)\,\phi_\alpha(x). \tag{39}$$

Here the eigenvalue ζ_α and the eigenfunction ϕ_α are the solution of the following integral equation,

$$\int_{-1}^{1}dx_2\{-A_1(x_1,x_2)\}\,\phi_\alpha(x_2)=\zeta_\alpha\phi_\alpha(x_1). \tag{40}$$

We note that $\chi^{KK}(q)$ shows a maximum at $q=0$. The associated correlation length ξ^{KK} is defined in the same way as ξ.

By using the numerical solutions of the integral equations (10), (25), (26), and (40), we will obtain the numerical results for thermodynamic quantities, which will be presented in the next section.

3. Results and discussion

In the previous section, all thermodynamic quantities were given in terms of the eigenvalues and the eigenfunctions of three kinds of the integral equations. We adopt the 24-point Gaussian integration formula to solve them and to perform integrations [6]. The accuracy of our results depends on the accuracy of our numerical solutions for the integral equations. At some points in the parameter space, we compare the results with those obtained by using the 40-point Gaussian integration formula. Another check has also been made for the case of $j=0$, on which we can easily reproduce the exact result. These procedures confirm that errors are significant only below $t \leqq 0.04$. When values for the thermodynamic quantities can be evaluated at $t=0$, we use these to extrapolate our numerical values to $t=0$; otherwise we extrapolate to $t=0$ rather arbitrary.

We show first in Fig. 2 the internal energy as a function of temperature. The internal energies increase from their zero temperature values

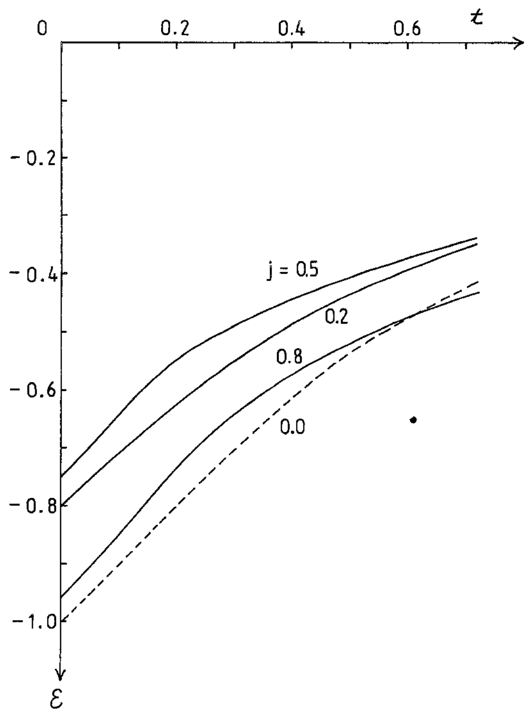

Fig. 2. Internal energy versus temperature for different values of j. Note that for $j>1/4$ the ground state is helimagnetic while for $j \leqq 1/4$ it is antiferromagnetic

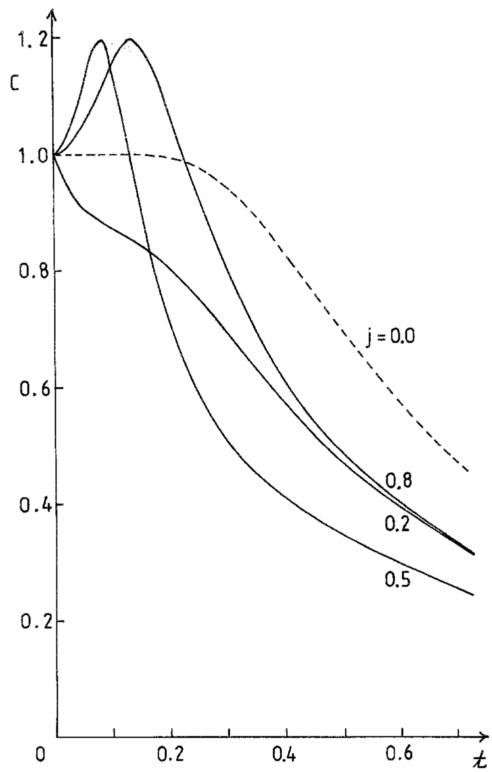

Fig. 3. Heat capacity versus temperature for different values of j. Note the peak at low temperatures for the cases of $j=0.5$ and 0.8, where the helical short-range order dominates

($\varepsilon(t=0)=-1+j$ for $j \leqq 1/4$ and $\varepsilon(t=0)=-1/8j-j$ for $j>1/4$) with finite slopes. This fact relates to the finite values of the heat capacity at zero temperature (see Fig. 3) and comes from the classical nature of our model. In real materials the quantum nature of spins affects thermodynamics at low temperatures so that $C \to 0$ as $t \to 0$. The most significant feature seen in the heat capacity versus temperature curves is the strong peak for $j>1/4$. Recalling the results of the planar model [4], we attribute it to the presence of chiral domain walls. However, in the present case, the effect of chiral domain walls is less pronounced than for the planar model. The reason probably is that the chirality vector K is a three dimensional vector so that its effect is more or less similar to that of the familiar excitations. This is contrasted with the case of the planar model, where K is pseudo-scalar and therefore introduces Ising type excitations into the system.

Next we present the results of the structure factor $S(q)$, which contain much more detailed information about the nature of the helical short-range order. As a consequence of the helical order $S(q)$ exhibits a maximum at $q = \pm q_m$ where q_m takes continuous values between π and $\pi/2$, depending on j. At $t=0$ q_m is equal to $Q=\arccos(-1/4j)$. The wave-number q_m de-

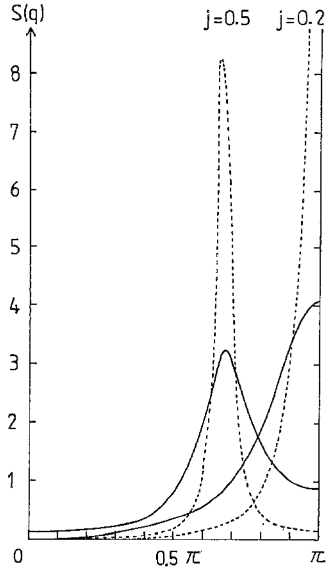

Fig. 4. Fourier-transformed spin correlation function for different temperatures; the dotted lines represent the result for $t=0.05$ and the solid lines show that for $t=0.2$. Note that the peak occurs at $2\pi/3$ for $j=0.5$ while it occurs at π for $j=0.2$

pends also on the temperature but the dependence is so weak that we can find no trace in Fig. 4, where some examples of $S(q)$ are presented. (This statement holds equally for other values of j.) This is in contrast with the strong temperature dependence in the planar model [4]. On the other hand, the maximum of $S(q)$ at $q=q_m$ tends to diverge at $t=0$, indicating the helical long-range order of our classical spin system. Another indication for the long-range order appears in Fig. 5, where the inverse of the correlation length $1/\xi$ tends to zero as $t\to 0$. To see the low temperature behavior in more detail, we tried to fit the calculated values of $1/\xi$ on the form, $1/\xi=f(t/\varepsilon_0)$, where ε_0 has been assumed to be the chiral domain wall energy, $\varepsilon_d=2j-1/8j$, which is estimated by assuming the simplest spin structure for the wall: Every spin in the left-hand side of the wall makes an angle Q with its nn spins and every spin in the right-hand side makes an angle $-Q$. As is seen in Fig. 5 all the values for different t and j fall reasonably on a single curve. Although it is difficult to determine the functional form of f in the whole range of t/ε_0, f can be fitted by the power law, $f(x)=cx$ for $x<0.08$. In addition, the correlation length of the chirality ξ^{KK}, shown in Fig. 6, obeys the same scaling law; however, ξ^{KK} is always about 30% shorter than ξ. These observations suggest that at such low temperatures the freedom of chirality is the only one to survive and dominate the thermodynamics.

The other point which we want to emphasize is the asymmetric shape of $S(q)$ for $j>1/4$. The shape for $j\leqq 1/4$ is symmetric around its maximum at $q=\pi$

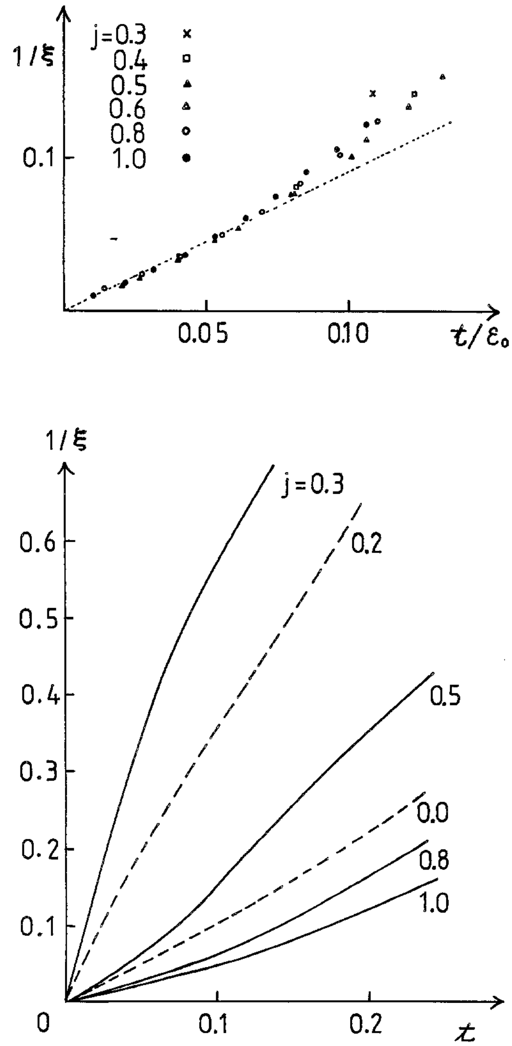

Fig. 5. Inverse correlation length versus temperature for different values of j, yielding the helical short-range order (the solid lines) and the antiferromagnetic short-range order (the dashed lines). The upper part shows scaling behavior

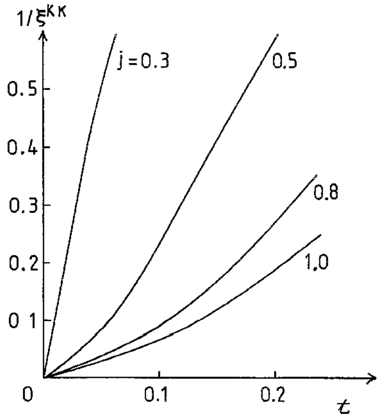

Fig. 6. Inverse correlation length of the chirality vector (see text) versus temperature for different values of j. Note that the chirality makes sense only in the helical short-range order phase

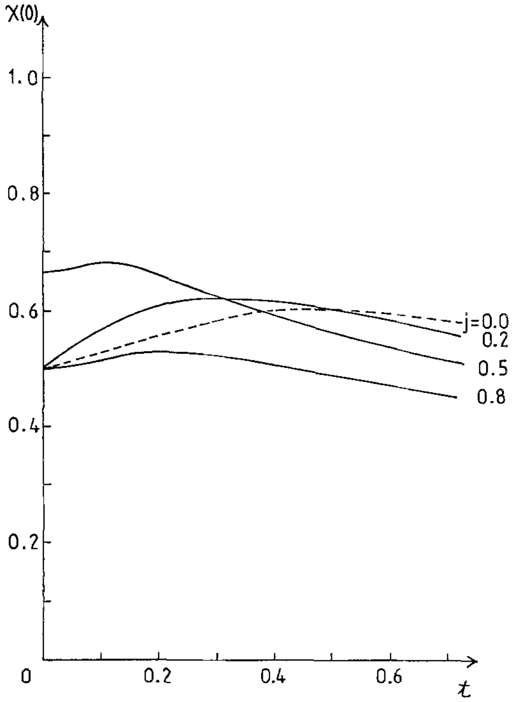

Fig. 7. Uniform susceptibility versus temperature for different values of j. Note that for $j > 1/4$ the ground state is helimagnetic while for $j \leqq 1/4$ it is antiferromagnetic

but, when j increases beyond 1/4, the maximum shifts towards lower value of q_m and the shape becomes asymmetric around $q = q_m$. These features already have been pointed out by De Raedt and De Raedt [3] with an explanation based on the spin wave dispersion curve. Here we want to emphasize again the important contribution from the chiral domain wall: For $J_1, J_2 > 0$ the domain wall including the antiferromagnetic point ($q = \pi$) is more likely than that including the ferromagnetic point ($q = 0$) and hence $S(q)$ is larger on the high q side of the maximum than on the low q side.

Based on these findings we conclude with the following conjecture. At $t = 0$ spins are aligned in parallel planes making an angle Q (or $-Q$) with their nn spins, although the plane can be chosen arbitrary. When t is increased some excitations appear in the system. It is natural to consider the local fluctuation of the helical plane, which leads to the chiral domain wall. We emphasize that these fluctuations do not affect so seriously the nn spin correlation since even at the center of the wall spins can keep the angle almost the same as that in the bulk. This is an important difference of the chiral domain wall from that in the planar model. Roughly speaking, q_m corresponds to the averaged angle between nn spins and hence it is consistent with the fact that q_m does not depend crucially on the temperature. On the other hand these excitations affect the heat capacity and the chiral susceptibility, on which we have found the effects of these excitations. When t is increased more the chirality looses its meaning. It is noted that the characteristic energy of these excitations are much smaller than the typical energy of the system, for example the nn interaction.

Finally, we present the result of the uniform susceptibility in Fig. 7. For $j = 0$ the susceptibility shows a broad maximum at $t \cong 0.5$. This maximum shifts towards lower temperature as j increases from zero but around $j = 0.4$ it turns to shift towards higher temperature. This is due to a competition between nn and nnn exchange interactions but no other significant behavior caused by the helical short-range order is found.

4. Conclusion

In this paper, we have developed the transfer matrix method for the Heisenberg chain to allow to include the nnn interaction. The thermodynamic quantities have been given in terms of the eigenvalues and the eigenfunctions of integral equations; these have been solved numerically with the aid of the Gaussian integration formula. Numerical results reveal characteristic effects of the helical short-range order. Especially in the structure factor $S(q)$ we have found that for $j \geqq 1/4$ a maximum occurs at $q = \pm q_m$ with asymmetric shape around the maximum. These findings are similar to those for a helical chain in the planar model, but the following points are different: *(1)* The characteristic wave number q_m shows no appreciable temperature dependence and *(2)* the correlation length tends to diverge as $1/t$ at very low temperatures. These differences have been attributed to the different nature of the chiral domain walls in the two system, being important excitations at low temperatures.

At last we want to comment on the experimental results for the quasi-one-dimensional magnet, $FeMgBO_4$, in which the nnn interaction has the same order of magnitude as the nn interaction because of the zig-zag form of the magnetic chains [7, 8]. Qualitative features of the experimental results for the susceptibility and the spin correlation functions seem to be reproduced correctly by our calculations. For a quantitative comparison, however, it is necessary to take into account of the nonmagnetic-impurity effect because this material contains an inevitable site inversion between Fe^{3+} and Mg^{2+}. Further, it may turn out necessary to consider the anisotropy. It is an interesting problem to study the anisotropic Heisenberg model which interpolates the two helical models, the planar model and the isotropic Heisenberg model.

This work has been funded by the German Federal Minister for Reseach and Technology (BMFT) under contract number 03-MI-1HAN-6. The numerical calculations were performed at the Regionales Rechenzentrum für Niedersachsen, Hannover.

References

1. Tonegawa, T., Harada, I.: J. Phys. Soc. Jpn. **56**, 2153 (1987)
2. Harada, I., Kimura, T., Tonegawa, T.: J. Phys. Soc. Jpn (to be published)
3. De Raedt, H., De Raedt, B.: Phys. Rev. B **19**, 2595 (1979)
4. Harada, I.: J. Phys. Soc. Jpn. **53**, 1643 (1984)
5. Takagi, Y.: MC Thesis, Kobe Univercity, 1981 (unpublished)
6. Blume, M., Heller, P., Lurie, N.: Phys. Rev. B **11**, 4483 (1975)
7. Wiedenmann, A., Burlet, P.: J. Phys. (Paris) **39**, 8-6C, 720 (1978)
8. Wiedenmann, A., Burlet, P., Scheuer, H., Convert, P.: Solid State Commun. **38**, 129 (1981)

I. Harada
Department of Physics
Faculty of Science
Kobe University
Rokkodai
Kobe/657 Japan

H.J. Mikeska
Institut für Theoretische Physik
Universität Hannover
Appelstrasse 2
D-3000 Hannover 1
Federal Republic of Germany